Materials Advances

ROYAL SOCIETY OF CHEMISTRY

PAPER

View Article Online
View Journal | View Issue

Cite this: *Mater. Adv.*, 2025, **6**, 8930

Local structure, zero field splitting and optical absorption of Mn^{2+} doped $ZnK_2(SO_4)_2{\cdot}6H_2O$ single crystals

Maroj Bharati, [a] Vikram Singh [a] and Ram Kripal *[b]

Received 30th August 2025,
Accepted 30th September 2025

DOI: 10.1039/d5ma00984g

rsc.li/materials-advances

The Mn^{2+} doped $ZnK_2(SO_4)_2{\cdot}6H_2O$ (ZKS) single crystal zero field splitting parameters are obtained using the superposition model. The evaluated parameters agree well with those found from EPR. The conclusion of the experiment that in ZKS, the Mn^{2+} ion takes the place of the Zn^{2+} site is verified by theoretical analysis. The crystals' optical spectra are estimated by utilizing the crystal field parameters obtained from the superposition model and the crystal field analysis computer program. A good agreement between the calculated and experimental band positions is found. Thus, the experimental results are confirmed by the theoretical studies.

1. Introduction

The EPR of the Mn^{2+} impurity has been widely studied in a variety of single crystals due to the sensitivity of its zero field splitting values to small structural distortions in the lattice.[1,2] A number of studies have been reported on impurities doped into diamagnetic host lattices at room temperature.[3–5]

The superposition model (SPM) can be used to model the zero field splitting (ZFS) and crystal field (CF) parameters for use in other studies.[6–10] SPM and the point-charge model[11–13] are commonly used to determine the parameters of the crystal field (CF). SPM was proposed for CF under certain assumptions.[14] (1) The CF at a paramagnetic ion is expressible as an algebraic sum of contributions, from other ions in the crystal. (2) When the paramagnetic ion is located at the origin of a chosen coordinate frame, all the major CF contributions from every single ion in the crystal are axially symmetric with respect to its position vector. (3) Only neighboring or coordinated ions (ligands) need to be counted for their CF contributions. (4) CF contributions from single ligands are transferable across different host crystals. Finding a steady spherical polar coordinate system (R_L, θ_L, Φ_L) for each ligand or ion from the host crystal's X-ray data is crucial for carrying out an SPM analysis on the CF. Ionic charge, ionic size, and inter-ionic bonding mismatches are likely to cause some local distortion when transition metal ions are infused. Critical analysis of the experimental spin-Hamiltonian parameters for Mn^{2+} and Fe^{3+} in CaO and MgO crystals has been done[15] providing the SPM parameters for the EPR data and showing that the CF for 3d ions satisfies the superposition principle. For the alkali earth oxides, sets of SPM intrinsic parameters based on reliable ligand distances have been determined.[16]

The crystals with the general formula $A_2^{+}B^{2+}(XO_4)_2{\cdot}6H_2O$ are known as Tutton single crystals, where A is a monovalent cation, B is a divalent cation usually a transition metal and X can be sulfur or selenium.[17,18] Tutton salts are a famous isostructural crystal family which shares the same monoclinic symmetry and the space group $P2_1/a$ with two formula units per unit cell $Z = 2$.[19] The Tutton salts are valuable crystals as they are used extensively in UV filters.[20]

Zinc potassium sulfate hexahydrate crystals (ZKS) are crystallized in the monoclinic crystal system and belong to the Tutton crystalline salts. These crystals, because of their growth with high purity and suitable crystal sizes and small transparency in the UV region, could be potential candidates for optoelectronic applications.[21]

EPR study of Mn^{2+} doped ZKS has been done at 293.7 K and the spin-Hamiltonian parameters have been obtained.[22] From angular variation studies, it is determined that magnetic $[Mn(H_2O)_6]^{2+}$ complexes are created when the Mn^{2+} ion enters the divalent sites of the Tutton salt lattice. The a^*bc axis system, where b and c are the crystal axes and a^* is perpendicular to b and c, is used to discuss the orientations. The EPR x and z axes deviate by 9° from both the Zn–O(7) and Zn–O(9) directions in ZKS.

The density functional theory (DFT) studies elucidate the electronic structure regulation in Ru–$NiCo_2O_4$ and the

[a] *Department of Physics, Nehru Gram Bharti (DU), Jamunipur, Prayagraj 221505, Uttar Pradesh, India. E-mail: marojbharati99@gmail.com, vikram.singh@ngbu.edu.in; Fax: +91-532-2460993; Tel: +91-532-2470532, +91-7459810790, +91-9450254530*

[b] *EPR Laboratory, Department of Physics, University of Allahabad, Prayagraj-211002, Uttar Pradesh, India. E-mail: ram_kripal2001@rediffmail.com; Tel: +91-9935080682*

modification of the d-band center optimizes H* adsorption energy, which considerably increased the hydrogen production efficiency.[23] A Mo-doped CoN is coupled with NiFe-LDH for preparing a Mott–Schottky heterojunction, addressing the enhanced hydrogen evolution reaction (HER), oxygen evolution reaction (OER), and urea oxidation reaction (UOR) compared with the individual counterparts.[24] This process for varying the local electron density could be a promising route to obtain low-energy consumption green hydrogen generation. DFT calculations were performed to further understand the catalytic mechanism and to assess the influence of Mo doping and heterointerfaces on the HER and OER performance of Mo–CoN coupled with NiFe-LDH. The incorporation of Mo and the fabrication of the composite with NiFe-LDH improve the electrocatalytic activity by modulating the electronic structure [JEC]. The above studies motivated us to perform a theoretical study on the local structure, zero field splitting and optical absorption of Mn^{2+} doped ZKS.

In this study, the ZFS parameters D and E are determined for the Mn^{2+} ion in ZKS at 293.7 K (room temperature, RT) taking CF parameters obtained from SPM and perturbation equations.[25] The goal is to locate the Mn^{2+} ion and the distortion that is taking place in the ZKS crystal. The results obtained for the Mn^{2+} ion at the substitutional Zn^{2+} site in the ZKS crystal with local distortion show good agreement with the EPR experimental values. The crystal field analysis (CFA) program and CF parameters are used to calculate the optical spectra of the Mn^{2+} doped ZKS single crystals. The calculated positions of the optical energy bands agree reasonably well with those obtained from the experiment. A further aim of the study is to find the extent to which CF theory and SPM analysis can be applied to Mn^{2+} ions in ZKS crystals in order to generate an SPM parameter database. This will determine molecular nanomagnet (MNM) design and computer simulation of their magnetic and spectroscopic characteristics. The transition ion-based MNM class currently includes single-molecule magnets (SMMs),[26] single-chain magnets (SCMs),[27] and single ion magnets (SIMs).[28] Because of the interesting magnetic properties of MNMs, such as magnetization's macroscopic quantum tunneling and possible uses in high-density information storage and quantum computing, the above systems have attracted large attention from scientists and researchers.[26,27] There are several synthesized SCM or SMM systems with Mn^{2+} and Cr^{3+} ions.[29] Since model calculations for simpler crystal systems can be used as a basis for more complex ones, the parameters of the model obtained in this case may be used for ZFS parameter calculations for Mn^{2+} ions at similar sites in MNM. This work's modeling can be extended to investigate various crystals of scientific and industrial interest in a number of other ion-host systems.

2. Crystal structure

The crystal structure of Tutton salt ZKS is monoclinic with space group $P2_1/a$.[21,30] The unit cell's parameters are as follows: $Z = 2$, $\beta = 104.78^\circ$, $a = 9.044$, $b = 12.194$ and $c = 6.151$ Å. All other

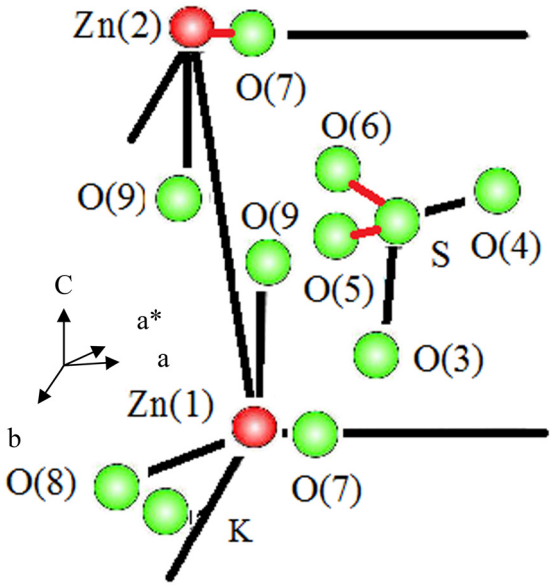

Fig. 1 The room-temperature ZKS crystal structure and the symmetry-adopted axis system (SAAS).

divalent cations in the unit cell are in general positions, with the two inequivalent ones located at points (0, 0, 0) and (1/2, 1/2, 0). Each divalent cation is surrounded by a slightly distorted octahedron of water molecules.[30] Fig. 1 shows the symmetry adopted axis system (SAAS) and ZKS crystal structure.

3. Crystal field and zero field splitting parameter calculations

The EPR spectra can be analyzed with the spin Hamiltonian:[7]

$$E\left(S_x^2 - S_y^2\right) + D\left\{S_z^2 - \frac{1}{3}S(S+1)\right\} + \mu_B B \cdot g \cdot S = \mathcal{H} \quad (1)$$

where B, μ_B, g, D and E are the applied magnetic field, Bohr magneton, splitting factor, second rank axial, and second rank rhombic ZFS parameters.[31,32] The modified crystallographic a^*, b and c axes (a^* is normal to axes b and c) and the (x, y, z) laboratory axes are shown in Fig. 1. The directions of metal–ligand bonds being mutually perpendicular are referred to as the symmetry adopted axes (SAA) or the local symmetry axes of the site. As shown in Fig. 1, the axis-Z of SAAS is along the crystal axis-c, and (X, Y) are perpendicular to the axis-Z. When Mn^{2+} ions are introduced in the ZKS crystal, they substitute at Zn^{2+} (1) sites with some local distortion in the lattice.[33]

The Mn^{2+} ion spin Hamiltonian can be written as,[34]

$$\mathcal{H} = \mathcal{H}_o + \mathcal{H}_{so} + \mathcal{H}_{ss} + \mathcal{H}_c \quad (2)$$

$$\mathcal{H}_c = \sum B_{kq} C_q^{(k)} \quad (3)$$

where B_{kq}, in Wybourne notation, represent the CF parameters and $C_q^{(k)}$, the spherical tensor operators. $B_{kq} \neq 0$ in the orthorhombic symmetry crystal field only for $k = 2, 4$; $q = 0, 2, 4$. Employing SPM, the CF parameters B_{kq} are computed.[34]

The symmetry of the local field about Mn^{2+} ions in the ZKS crystal is taken to be orthorhombic (OR-type I),[7] where the ZFS parameters D and E are found as follows:[35]

$$D = \left(\frac{3\varsigma^2}{70P^2D'}\right)\left[-B_{20}{}^2 - 21\varsigma B_{20} + 2B_{22}{}^2\right] + \left(\frac{\varsigma^2}{63P^2G}\right)\left[-5B_{40}{}^2 - 4B_{42}{}^2 + 14B_{44}{}^2\right] \quad (4)$$

$$E = \left(\frac{\sqrt{6}\varsigma^2}{70P^2D'}\right)[2B_{20} - 21\varsigma]B_{22} + \left(\frac{\varsigma^2}{63P^2G}\right)\left[3\sqrt{10}B_{40} + 2\sqrt{7}B_{44}\right]B_{42} \quad (5)$$

Here $P = 7B + 7C$, $G = 10B + 5C$, $D' = 17B + 5C$. B and C represent Racah parameters and ς is the spin–orbit coupling parameter. In terms of average covalency parameter N, $B = N^4B_0$, $C = N^4C_0$, $\varsigma = N^2\varsigma_0$, where ς_0 gives the free ion spin–orbit coupling parameter and B_0 and C_0 are Racah parameters for the free ion.[34,36] $\varsigma_0 = 336\ cm^{-1}$, $B_0 = 960\ cm^{-1}$ and $C_0 = 3325\ cm^{-1}$ for free Mn^{2+} ions.[7]

The covalency parameter N is found from $N = \left(\sqrt{\frac{B}{B_0}} + \sqrt{\frac{C}{C_0}}\right)\Big/2$ using Racah parameters ($B = 850\ cm^{-1}$, $C = 2970\ cm^{-1}$) obtained from optical analysis of the Mn^{2+} ion in zinc cesium sulphate hexahydrate where ligands are oxygens,[37] as no optical absorption of Mn^{2+} doped ZKS has been reported.

The CF parameters using SPM are determined,[14,35] in terms of co-ordination factor $K_{kq}(\theta_j,\varphi_j)$ and intrinsic parameter $\overline{A_k}(R_j)$, as

$$B_{kq} = \sum_j \overline{A_k}(R_j)K_{kq}\left(\theta_j, \varphi_j\right) \quad (6)$$

$\overline{A_k}(R_j)$ is found from

$$\overline{A_k}(R_0)\left(\frac{R_0}{R_j}\right)^{t_k} = \overline{A_k}(R_j) \quad (7)$$

where the ligand's distance from the d^n ion is denoted by R_j, $\overline{A_k}(R_0)$ is the intrinsic parameter, R_0 is the reference distance of the ligand from the metal ion and t_k gives the power law exponent. For Mn^{2+} doped crystals, $t_2 = 3$ and $t_4 = 7$ were used earlier,[35] the same values are taken here. Since the co-ordination about the Mn^{2+} ion is octahedral, $\overline{A_4}$ is obtained from the relation[38]

$$\overline{A_4}(R_0) = \frac{3}{4}Dq \quad (8)$$

From optical study,[37] $Dq = 790\ cm^{-1}$. Therefore, $\overline{A_4}(R_0) = 592.5\ cm^{-1}$. For $3d^5$ ions the ratio $\frac{\overline{A_2}}{\overline{A_4}}$ falls in the range 8–12.[34,39,40] With $\overline{A_2} = 10\overline{A_4}$, $\overline{A_2} = 5925\ cm^{-1}$.

4. Results and discussion

Using SPM and the ligand configuration about the Mn^{2+} ion shown in Fig. 1, the CF parameters of the Mn^{2+} ion at the Zn^{2+} (1) sites are estimated. Table 1 provides atoms' coordinates in the ZKS single crystal with bond length R (both with and without distortion) and angles θ, φ for site I. The ZFS and CF parameters together with reference distance R_0 are presented in Table 2. Table 2 shows that $R_0 = 0.200$ nm, being slightly less than the sum of the radii of the ions (0.223 nm) of $Mn^{2+} = 0.083$ nm and $O^{2-} = 0.140$ nm with no distortion and $\frac{\overline{A_2}}{\overline{A_4}} = 8, 10, 12$ provide ZFS parameter values at octahedral substitutional site I different from the EPR experimental ones.[22] Experimental parameters of ZFS $|D|$ and $|E|$ (in unit of $10^{-4}\ cm^{-1}$) for site I from EPR are 355.8, 57.2, respectively. $|E|/|D|$ is obtained as 0.160 being smaller than the standard value 0.33.[32] $|D|$ and $|E|$ estimated theoretically without distortion are larger than the EPR experimental values. The value of $|E|/|D|$ is also larger than the standard value 0.33.[32] Therefore, local distortion is included into the calculation. For local distortion an iterative procedure has been used by changing R, θ and φ to minimize the difference between calculated and experimental D and E and E/D near to

Table 1 Atoms' coordinates, bond length R (both with and without distortion) and angles θ, φ in the ZKS single crystal (site I)

					Spherical polar coordinates of ligands					
Mn^{2+} position	Ligands	x (Å)	y (Å)	z (Å)	R (nm)		θ°		φ°	
Without distortion										
Site: substitutional	O7	0.1723	0.1080	0.1683	0.20741	R_1	85.34	θ_1	85.22	φ_1
Zn(1)	O8	−0.1629	0.1113	0.0351	0.20598	R_2	89.02	θ_2	94.53	φ_2
(0.0000, 0.0000, 0.0000)	O9	−0.0007	−0.0676	0.3024	0.20362	R_3	81.46	θ_3	90.02	φ_3
	O7′	−0.1723	−0.1080	−0.1683	0.20741	R_4	94.65	θ_4	94.78	φ_4
	O8′	−0.1723	0.3920	0.6683	0.67733	R_5	84.34	θ_5	91.46	φ_5
	O9′	0.1723	0.6080	0.3317	0.77278	R_6	87.54	θ_6	88.72	φ_6
With distortion										
I	O7				0.28741		66.34		86.72	
	O8				0.28598		70.02		92.53	
	O9				0.26007		62.46		88.02	
	O7′				0.30901		86.65		90.78	
	O8′				0.79733		82.34		91.46	
	O9′				0.85778		89.54		90.72	

Table 2 The Mn^{2+} doped ZKS crystal's CF and ZFS parameters

	Crystal-field parameters (cm^{-1})						Zero-field splitting parameters ($\times 10^{-4}$ cm^{-1})		
Site	R_0 (nm)	B_{20}	B_{22}	B_{40}	B_{42}	B_{44}	$\|D\|$	$\|E\|$	$\|E\|/\|D\|$
Without distortion site I									
$\frac{\overline{A_2}}{\overline{A_4}} = 8$	0.200	−17 062.3	−21 071.6	5249.723	5583.833	8072.755	3295.6	1679.4	0.509
$\frac{\overline{A_2}}{\overline{A_4}} = 10$	0.200	−21 327.9	−26 339.5	5249.723	5583.833	8072.755	4724.9	2421.1	0.512
$\frac{\overline{A_2}}{\overline{A_4}} = 12$	0.200	−25 593.5	−31 607.4	5249.723	5583.833	8072.755	6458.7	3314.3	0.513
With distortion site I									
$\frac{\overline{A_2}}{\overline{A_4}} = 8$	0.200	−5618.94	2495.683	−133.084	−19.7999	2948.929	285.2	75.7	0.265
$\frac{\overline{A_2}}{\overline{A_4}} = 10$	0.200	−7023.67	3119.604	−133.084	−19.7999	2948.929	355.8	109.3	0.307
Exp.							355.8	57.2	0.160
$\frac{\overline{A_2}}{\overline{A_4}} = 12$	0.200	−8428.4	3743.524	−133.084	−19.7999	2948.929	437.7	148.9	0.340

standard value 0.33[32] keeping in mind the minimum lattice strain. Using the above value of R_0 and local distortion, the ZFS parameters for substitutional octahedral sites I are determined for $\frac{\overline{A_2}}{\overline{A_4}} = 8, 10, 12$ and are given in Table 2. The ZFS parameter values are smaller than the experimental ones (error 19.84%) for $\frac{\overline{A_2}}{\overline{A_4}} = 8$ and larger for $\frac{\overline{A_2}}{\overline{A_4}} = 12$ (error 23.02%, $|E|/|D|$ is also larger than the standard value 0.33) while these are in good agreement with the EPR experimental values for $\frac{\overline{A_2}}{\overline{A_4}} = 10$.[22] Hence $\frac{\overline{A_2}}{\overline{A_4}} = 10$ seems to be appropriate. The parameters $t_2 = 3$ and $t_4 = 7$ with transformation S2 for standardization[32] are employed to get an $|E|/|D|$ ratio near to 0.33 and calculated ZFS parameters close to the experimental values from EPR. A similar value of $\frac{\overline{A_2}}{\overline{A_4}}$ has been used for Mn^{2+} doped diglycine calcium chloride tetrahydrate[41] and Fe^{3+} doped $BiVO_4$.[34]

The CFA program[42] and B_{kq} parameters (with distortion) are used to calculate the optical spectra of Mn^{2+} doped ZKS single crystals. By diagonalizing the full Hamiltonian, the positions of the energy bands of the Mn^{2+} ion are evaluated. Table 3 shows the energy band positions (experimental and calculated) for substitutional site I.[37] From the position and the nature of the bands observed, they have been ascribed to a Mn^{2+} ion in octahedral symmetry.[37,43] Ligand field bands are sharp when the energy expressions for the transitions are independent of Dq, since the number of t_{2g} electrons is the same in both the excited and the ground states.[43] The sharp bands are therefore assigned to the [$^4A_{1g}$(G), ^4E_g(G)] and the ^4E_g(D) states, respectively. The broad bands are assigned to $^4T_{1g}$(G) and $^4T_{2g}$(G), respectively. These bands are broad as their transitions involve a change of configuration from $(t_{2g})^3(e_g)^2$ to $(t_{2g})^4(e_g)$. The remaining bands are assigned to $^4T_{2g}$(G), $^4T_{1g}$(P) and $^4T_{1g}$(F) states, respectively. The CFA program[42] can perform diagonalization of the complete Hamiltonian within the $3d^N$ basis of states in the intermediate crystal field coupling scheme providing not only the CF energy levels but also the state vectors. The Hamiltonian incorporated in the CFA program contains the Coulomb interaction (in terms of the Racah parameters B and C), Trees correction (α), the spin–orbit interaction (ζ), the crystal field Hamiltonian, the spin–spin interaction (M_0), and the spin-other orbit interaction (two parameters: M_{00}, M_{22}). The adjusted values of the free-ion parameters used in the CFA calculations are (in cm^{-1}): $B = 850$ and $C = 2970$, $\alpha = 76$, $\zeta_0 = 336$ cm^{-1}, $M_0 = 0.2917$, $M_2 = 0.0229$, $M_{00} = 0.2917$, and $M_{22} = 0.0229$. Though the whole Mn^{2+} spectra consist of 120 degenerate states, we present only a few energy levels based on intensity.[44] The transitions associated with ^4E_g(G), $^4A_{1g}$(G), $^4T_{2g}$(D), ^4E_g(D) and $^4A_{2g}$(F) are well predicted while the transitions associated with $^4T_{1g}$(G), $^4T_{2g}$(G), $^4T_{1g}$(P) and $^4T_{1g}$(F) show larger deviation. The reasons for these deviations may be electron correlation effects, vibronic coupling or limitations of the CF model.[33]

Table 3 Both calculated and experimental energy bands of the single crystal of ZKS doped Mn^{2+}

Transition from $^6A_{1g}$(S)	Observed band (cm^{-1})	Calculated band (cm^{-1}) I
$^4T_{1g}$(G)	18 436	23 327, 23 343, 23 513, 23 592, 23 759, 23 843
$^4T_{2g}$(G)	22 815	23 979, 24 000, 24 363, 24 402, 24 445, 24 485
^4E_g(G)	24 783	24 828, 24 856, 24 865, 24 872
$^4A_{1g}$(G)	24 850	24 880, 24 889
$^4T_{2g}$(D)	28 003	26 582, 26 639, 27 214, 27 274, 28 565, 28 578
^4E_g(D)	29 870	29 249, 29 305, 29 730, 29 828
$^4T_{1g}$(P)	32 435	31 477, 31 502, 34 913, 35 045, 35 148, 35 264
$^4A_{2g}$(F)		36 656, 36 961
$^4T_{1g}$(F)	41 460	40 843, 40 559, 40 678, 40 730, 40 790, 40 799

It is evident from Table 3 that the calculated and experimental energy band positions agree fairly well. Therefore, the theoretical results verify the EPR experimental one[22,37] that Mn^{2+} ions enter the ZKS crystal at the substitutional Zn^{2+} (1) octahedral site. The model parameters determined may be utilized in ZFS parameter estimations for Mn^{2+} ions at similar molecular nanomagnet sites.

5. Conclusions

To determine the zero field splitting parameters, the superposition model and perturbation theory are utilized for ZKS single crystals infused with Mn^{2+} ions. The calculated ZFS parameters match well with the experimental values from EPR for $\frac{\overline{A_2}}{A_4} = 10$. The computed optical spectra are discussed. The calculated positions of the optical energy bands agree reasonably well with those obtained from the experiment. Thus, the experimental result is supported by the theoretical analysis that Mn^{2+} ions substitute at Zn^{2+} (1) sites in ZKS. The model parameters evaluated in this study may be utilized for ZFS parameter determinations for Mn^{2+} ions at similar sites in MNM. The present modeling technique may be useful in finding various crystals of a number of scientific and industrial applications.

Ethical approval

There were no human or animal subjects in this study, and it wasn't conducted in any protected or private locations. Corresponding locations did not require any special permissions.

Author contributions

Vikram Singh and Maroj Bharati prepared the figure, wrote the manuscript, and carried out the computations. Ram Kripal: concept and oversight. The manuscript has been reviewed by all authors.

Conflicts of interest

The authors affirm that no known conflicting financial interests or personal relationships could have influenced any of the work presented in this paper.

Data availability

Data will be made available on request.

Acknowledgements

The authors are grateful to the Head of Physics Department of Allahabad University, Allahabad for giving facilities of the department and to Prof. C. Rudowicz of Faculty of Chemistry, Adam Mickiewicz University, Poznan, Poland for the CFA program.

References

1 J. Gtjens, M. Sjdin, V. L. Pecoraro and S. Un, The Relationship between the Manganese(II) Zero-Field Interaction and Mn(II)/Mn(III) Redox Potential of Mn(4′-X-terpy)$_2$ Complexes, *J. Am. Chem. Soc.*, 2007, **129**, 13825–13827.

2 D. P. Padiyan, C. Muthukrishnan and R. Murugesan, Single crystal EPR studies on Mn(II)-doped sarcosine cadmium chloride and sarcosine cadmium bromide: Study of zero-field splitting tensor in iso-structural complexes, *Spectrochim. Acta, Part A*, 2002, **58**, 509–517.

3 J. A. Weil and J. R. Bolton, *Electron Paramagnetic Resonance: Elementary Theory and Practical Applications*, Wiley, New York, 2nd edn, 2007.

4 S. P. Rathee and S. S. Hooda, EPR and superposition-model analysis of zero-field splitting parameters for Mn^{2+} doped in $ZnNbOF_5{\cdot}6H_2O$ and $CoNbOF_5{\cdot}6H_2O$ single crystals, *Indian J. Phys.*, 2025, **99**(1), 145–148.

5 D. Halder, Y. Jana, D. Piwowarska, P. Gnutek and C. Rudowicz, Tailoring single-ion magnet properties of coordination polymer $C_{11}H_{18}DyN_3O_9$ (Dy-CP) using the radial effective charge model (RECM) and superposition model (SPM), *Phys. Chem. Chem. Phys.*, 2024, **26**, 19947–19959.

6 C. Rudowicz, P. Gnutek and M. Açıkgöz, Superposition model in electron magnetic resonance spectroscopy – a primer for experimentalists with illustrative applications and literature database, *Appl. Spectrosc. Rev.*, 2019, **54**, 673–718.

7 A. Abragam and B. Bleaney, *Electron Paramagnetic Resonance of Transition Ion*, Dover, New York, 1986.

8 J. R. Pilbrow, *Transition-Ion Electron Paramagnetic Resonance*, Clarendon Press, Oxford, 1990.

9 B. G. Wybourne, *Spectroscopic Properties of Rare Earth*, Wiley, New York, 1965.

10 J. Mulak and Z. Gajek, *The Effective Crystal Field Potential*, Elsevier, Amsterdam, 2000.

11 R. Boča, Zero-field splitting in metal complexes, *Coord. Chem. Rev.*, 2004, **248**, 757–815.

12 Y. Y. Yeung, in *Optical Properties of 3d-Ions in Crystals: Spectroscopy and Crystal Field Analysis*, ed., M. G. Brik and N. M. Avram, Springer, Heidelberg, 2013, ch. 3, pp. 95–121.

13 A. K. Yadav, U. M. Tripathi and R. Kripal, Theoretical Calculation of Zero-Field Splitting Parameters for Mn^{2+} in Potassium Hydrogen Sulphate, *Appl. Magn. Reson.*, 2022, **53**, 941–947.

14 D. J. Newman and B. Ng, The superposition model of crystal fields, *Rep. Prog. Phys.*, 1989, **52**, 699–763.

15 D. J. Newman and E. Siegel, Superposition model analysis of Fe3+ and Mn2+ spin-Hamiltonian parameters, *J. Phys. C: Solid State Phys.*, 1976, **9**, 4285–4292.

16 Y. Y. Yeung, Local distortion and zero-field splittings of $3d^5$ ions in oxide crystals, *J. Phys. C: Solid State Phys.*, 1988, **21**, 2453–2462.

17 F. Bosi, G. Belardi and P. Ballirano, Structural features in Tutton's salts $K_2[M^{2+}(H_2O)_6](SO_4)_2$, with$M^{2+}$ = Mg, Fe, Co, Ni, Cu, and Zn, *Am. Mineral.*, 2009, **94**, 74–82.

18 M. Wildner, D. Marinova and D. Stoilova, Vibrational spectra of $Cs_2Cu(SO_4)_2{\cdot}6H_2O$ and $Cs_2Cu(SeO_4)_2{\cdot}nH_2O$($n$ = 4, 6) with a crystal structure determination of the Tutton salt $Cs_2Cu(SeO_4)_2{\cdot}6H_2O$, *J. Mol. Struct.*, 2016, **1106**, 440–451.

19 H. T. Montgomery and E. C. Lingafelter, The crystal structure of Tutton's salts. II. Magnesium ammonium sulfate hexahydrate and nickel ammonium sulfate hexahydrate, *Acta Crystallogr.*, 1964, **17**, 1478–1479.

20 M. de Oliveira, S. Ghosh, T. S. Pacheco, G. J. Perpétuo and C. J. Franco, Growth and structural analysis of ammonium nickel cobalt sulfate hexahydrate crystals, *Mater. Res. Express*, 2017, **4**, 105036.
21 A. Abu El-Fadl and A. M. Nashaat, Growth, structural, and spectral characterizations of potassium and ammonium zinc sulfate hydrate single crystals, *Appl. Phys. A: Mater. Sci. Process.*, 2017, **123**, 339.
22 S. J. Strach and R. Bramley, Zero-Field EPR of Mn^{2+} in Tutton Salts, *J. Magn. Reson.*, 1984, **56**, 10–32.
23 Y. Wang, L. Chen, H. Zhang, M. Humayun, J. Duan, X. Xu, Y. Fu, M. Bououdina and C. Wang, Elaborately tailored $NiCo_2O_4$ for highly efficient overall water splitting and urea electrolysis, *Green Chem.*, 2023, **25**, 8181–8195.
24 Z. Huang, J. Zhang, B. M. Humayunc,Y. Liu, W. Xiaoa, C. Fenga, K. Zhao, B. Wu,Y. Fua, M. Bououdinac, H. Zhang, G. Chen and C. Wang, Molybdenum-leveraged Mott–Schottky heterojunction for advanced water splitting and urea, electrolysis, *J. Energy Chem.*, 2025, **111**, 94–108.
25 W. L. Yu and M. G. Zhao, Spin-Hamiltonian parameters of ^6S state ions., *Phys. Rev. B: Condens. Matter Mater. Phys.*, 1988, **37**, 9254–9267.
26 G. Aromí and E. K. Brechin, Synthesis of 3d metallic single-molecule magnets, *Struct. Bonding*, 2006, **122**, 1–67.
27 C. Coulon, H. Misayaka and R. Clérac, Single-Chain Magnets: Theoretical Approach and Experimental Systems, *Struct. Bonding*, 2006, **122**, 163–206.
28 M. Murrie, Cobalt(II) single-molecule magnets, *Chem. Soc. Rev.*, 2010, **39**, 1986–1995.
29 C. van Wüllen, Magnetic anisotropy through cooperativity in multinuclear transition metal complexes: theoretical investigation of an anisotropic exchange mechanism, *Mol. Phys.*, 2013, **111**, 2392–2397.
30 H. Montgomery and E. C. Lingafelter, The Crystal Structure of Tutton's Salts. I. Zinc Ammonium Sulfate Hexahydrate, *Acta Crystallogr.*, 1964, **17**, 1295–1299.
31 C. J. Radnell, J. R. Pilbrow, S. Subramanian and M. T. Rogers, Electron paramagnetic resonance of Fe^{3+} ions in $(NH_4)_2SbF_5$, *J. Chem. Phys.*, 1975, **62**, 4948–4952.
32 C. Rudowicz and R. Bramley, On standardization of the spin Hamiltonian and the ligand field Hamiltonian for orthorhombic symmetry, *J. Chem. Phys.*, 1985, **83**, 5192–5197.
33 B. N. Figgis and M. A. Hitchman, *Ligand Field Theory and its Applications*, Wiley, New York, 2000.
34 T. H. Yeom, S. H. Choh, M. L. Du and M. S. Jang, EPR study of Fe^{3+} impurities in crystalline $BiVO_4$, *Phys. Rev. B: Condens. Matter Mater. Phys.*, 1996, **53**, 3415–3421.
35 T. H. Yeom, S. H. Choh and M. L. Du, A theoretical investigation of the zero-field splitting parameters for an Mn^{2+} centre in a $BiVO_4$ single crystal, *J. Phys.:Condens. Matter*, 1993, **5**, 2017–2024.
36 C. K. Jorgensen, *Modern Aspects of Ligand Field Theory*, North-Holland, Amsterdam, 1971, p. 305.
37 K. Purandar, J. L. Rao and S. V. J. Lakshman, Optical Absorption Spectrum of Mn^{2+} in Zinc Cesium Sulphte Hexahydrate, *Acta Phys. Slovaca*, 1984, **34**, 195–207.
38 *Crystal Field Handbook*, ed. D. J. Newman and B. Ng, Cambridge University Press, Cambridge, 2000.
39 A. Edgar, Electron paramagnetic resonance studies of divalent cobalt ions in some chloride salts, *J. Phys. C: Solid State Phys.*, 1976, **9**, 4303–4314.
40 R. Kripal, M. G. Misra, A. K. Yadav, P. Gnutek, M. Açıkgöz and C. Rudowicz, Theoretical Analysis of Crystal field Parameters and Zero field Splitting Parameters for Mn^{2+} ions in Tetramethylammonium Tetrachlorozincate, *Polyhedron*, 2023, **235**, 116341.
41 S. Pandey and R. Kripal, A Theoretical Analysis of Zero Field Splitting Parameters of Mn^{2+} Doped Diglycine Calcium Chloride Tetrahydrate, *Chin. J. Phys.*, 2014, **52**, 262–271.
42 Y. Y. Yeung and C. Rudowicz, Crystal Field Energy Levels and State Vectors for the $3d^N$ Ions at Orthorhombic or Higher Symmetry Sites, *J. Comput. Phys.*, 1993, **109**, 150–152.
43 Y. Tanabe and S. Sugano, On the Absorption Spectra of Complex Ions. I, *J. Phys. Soc. Jpn.*, 1954, **9**, 753–766.
44 Y. Y. Yeung, C. Rudowicz, Y. M. Chang and J. Qin, Model calculation of the spectroscopic properties for Cr^{3+} Kyanite, *J. Lumin.*, 1994, **60–61**, 108–111.